ARM: Anonymous Rating Mechanism for Discrete Power Control

Shuqin Li, *Member, IEEE*, Ziyu Shao, *Member, IEEE*, and Jianwei Huang, *Fellow, IEEE*

Abstract—Wireless interference management through continuous power control has been extensively studied in the literature. However, practical systems often adopt discrete power control with a limited number of power levels and MCSs (Modulation Coding Schemes). In general, discrete power control is NP-hard due to its combinatorial nature. To tackle this challenge, we propose an innovative approach of interference management: ARM (Anonymous Rating Mechanism). Inspired by the successes of the simple anonymous rating mechanism in E-commerce, we develop ARM as distributed near-optimal algorithm for solving the discrete power control problem (i.e., the joint scheduling, power allocation, and modulation coding adaption problem) under the physical interference model. We show that ARM achieves a close-to-optimal network throughput with a low control overhead. We also characterize the performance gap of ARM with the theoretical optimal solution due to the loss of rating information, and study the trade-off between such gap and the convergence time of ARM. We present numerical results with practical parameter choices to validate the theoretical findings, and highlight the impacts of approximation factor, the number of power levels, and the incomplete rating information.

Index Terms—Anonymous rating mechanism, Markov approximation, discrete power control

1 Introduction

Power control is a key tool in the management of wireless interference. Most of the existing results for wireless interference management assume a continuous space of power levels [2]. Under such a continuous power control setting, existing work can be divided into two main categories. One is concerned with achieving fixed Signal-to-Interference-plus-Noise-Ratio (SINR) targets [3], [4]. In this way, the link quality can be maintained at a desired target. A survey of related results can be found in [2]. The other is the joint SINR allocation and power control. This line of work often assumes that the link rate is a continuous function of the receiver SINR. A commonly used rate function is the Shannon capacity formula $r_l = B\log_2(1+\text{SINR}_l)$, where r_l is the rate of a link l, and B is the bandwidth. Under such settings, researchers have proposed both centralized algorithms (e.g., [2], [5]) and distributed approximation algorithms (e.g., [6], [7], [8]).

By comparing the key assumptions and results of the above literature with the practical systems, we have the following important observations.

First, the common assumption of continuous mapping from link rate to SINR level in [2], [5], [6], [7], [8] implies that for each SINR level, there is a MCS (modulation and coding scheme) available to achieve the corresponding channel capacity. This is often not the case in practice, as there are only a limited number of MCSs available. For example, there are only four modulations in LTE: BPSK, QPSK, 16QAM, and 64QAM, with limited choices of coding rates[9]. Under the setting of limited MCSs, Zhou et al. in [10] proposed a distributed near-optimal algorithm to solve the continuous power control problem. Such an algorithm induces high communication overheads, since it requires each link to obtain the global information for iterative updates. Furthermore, it is difficult to characterize the convergence time and impacts of various design parameters.

Second, and more importantly, we observe that only a limited number of power levels are used in practical systems [9]. For example, current 3GPP LTE standard of networks only supports discrete power control in the downlink via a user-specific data-to-pilot-power offset parameter [9], which chooses a baseline of power and four fixed power offset parameters for each link [9]. There are two main advantages of discrete power control compared to continuous power control. One is the simplified design of the transmitter, and the other is the massive reduction of the information exchange overhead within system, which further simplifies the system design. In our simulation studies related to discrete power control, we also observe that using a small number of power levels is able to achieve a close-to-optimal throughput (comparing with the optimal continuous power control benchmark) with light overhead of message exchanges. Further increasing the number of power levels can only have a marginal system performance improvement at the expense of a fast increasing implementation complexity.

Existing work on discrete power control (power control with discrete power levels) can also be divided into two categories. Most of them lie in the first category, which is concerned with achieving fixed Signal-to-Interference-plus-Noise-Ratio (SINR) targets by assuming either discrete power levels [11] or discrete power update step sizes [12]. A survey of these works can be found in [2]. The second

- *S. Li is with Bell Labs, Shanghai, China. E-mail: Shuqin.Li@alcatel-sbell.com.cn.*
- *Z. Shao is with the School of Information Science and Technology, ShanghaiTech University, Shanghai, China. E-mail: shaozy@shanghaitech.edu.cn.*
- *J. Huang is with the Department of Information Engineering, The Chinese University of Hong Kong, Shatin, Hong Kong. E-mail: jwhuang@ie.cuhk.edu.hk.*

Manuscript received 10 Aug. 2015; revised 13 Feb. 2016; accepted 25 Mar. 2016. Date of publication 31 Mar. 2016; date of current version 5 Jan. 2017. For information on obtaining reprints of this article, please send e-mail to: reprints@ieee.org, and reference the Digital Object Identifier below. Digital Object Identifier no. 10.1109/TMC.2016.2549007

1536-1233 © 2016 IEEE. Personal use is permitted, but republication/redistribution requires IEEE permission.
See http://www.ieee.org/publications_standards/publications/rights/index.html for more information.

category is our main focus, which is concerned with the rate maximization under the setting of discrete power levels [13], [14], [15], [16], [17], [18], [19], [20].

There are two main challenges of solving this rate-maximization problem. One is the computational complexity. This discrete power control problem is a combinatorial optimization problem and has been proved to be NP-hard [13], [14], hence is hard to solve even in a centralized fashion. The other is to have a good scalability for implementation in large-scale wireless networks. We need distributed implementations with low overhead of information exchanges.

Several works [13], [14], [15], [16], [17], [18], [19], [20] attempted to address the above challenges. Gjendemsjø et al. in [13] proposed a binary power allocation (BPA) algorithm for maximizing the total throughput, where each subchannel can either be silent or transmitting at maximum power. This algorithm requires global information to compute the transmit power and user assignment. Zhang et al. in [14] proposed two distributed iterative algorithms to maximize the weighted sum-rate in multi-cell networks, through discrete power allocation and coordinated scheduling. Both algorithms converge to some solutions without performance guarantees. Wang et al. in [15] applied an ant colony optimization technique to solve a discrete power allocation problem, obtaining a centralized solution without performance guarantees. Combes et al. in [16] proposed an online stochastic algorithm to maximize the expected number packets successfully sent over a given time horizon T. On the other hand, authors in [17], [18], [19], [20] adopted a game-theoretic formulation and proposed several stochastic learning algorithms, which converge to the desired equilibria under some limited conditions. However, all these works [13], [14], [15], [16], [17], [18], [19], [20] made an impractical assumption of continuous mapping from link rate to SINR level.

In this paper, however, we adopt a more practical setting including a limited number of power levels and MCSs (Modulation Coding Schemes), as well as discrete mapping from link rate to SINR level. To address the discrete power control problem with two main challenges under such a setting, we propose a distributed algorithm with provable near-optimal performance and light message exchange overhead.

The key component in our algorithm is the Anonymous Rating Mechanism (ARM), which is inspired by the anonymous rating mechanism widely used in today's online rating system. Examples of anonymous rating schemes include the "Like" of a post in Facebook (binary rating feedback), the voting score of a movie in IMDb (rating from zero to ten), and the rating of a product in Amazon (one to five stars). They are simple but informative for users to learn from others, find the good, and avoid the bad. If we imagine that users can continuously improve their choices based on others' ratings, then it may lead to a network-wide performance improvement. Motivated by this, we propose the ARM framework for wireless interference management. The key idea is to allow links to continuously rate their changes of transmission rate caused by the change of interference from their neighboring links. For example, a link will provide a five-star rating if its transmission rate increases significantly due to the decrease of its surrounding interference, and it will provide a one-star rating for a significant transmission rate drop. Based on all the feedback ratings from its neighbors, a link will smartly adapt its transmission power and MCS.

Our key results and contributions are summarized as follows:

- *Problem Formulation:* According to the best of our knowledge, this paper is the first to study the discrete power control problem with practical concerns of a limited number of power level and MCSs, as well as discrete mapping from link rate to SINR level. Such formulation considers joint scheduling, discrete power allocation, and modulation-coding adaptation under physical interference model.
- *Algorithm Design and Analysis:* We propose an ARM-based distributed algorithm with two variants to solve this problem, with provable near-optimal performance guarantees. One is with less performance but more robust, while the other is with better performance but less robust. We also characterize the key properties of the designed algorithms: approximation gap, perturbation error bound, convergence time, and trade-off between approximation gap and convergence time.
- *Robust Performance with Low Overhead:* Our algorithm allows distributed implementation with low message exchange overhead. Our algorithm is also robust to some rating information loss. We provide a bound of the induced optimality gap via perturbation analysis.
- *Simulation:* Extensive simulations based on practical system settings show that the performance gap between ARM and the optimal is small. Such a small gap can be achieved with only a small number of power levels, and the performance degradation is marginal if only limited local network information is available. We also provide performance comparisons between two variants of ARM.

The remainder of this paper is organized as follows. We introduce the system model and problem formulation in Section 2. Then we discuss design and analysis of the algorithm in Section 3. Performance evaluation is conducted in Section 4. We conclude this paper in Section 6. Due to the page limitation, we present some proof details in our technical report [21].

2 System Model and Problem Formulation

We consider a general wireless network consisting of a set of interfering *links* $\mathcal{L}$, where each link is a pair of transmitter and receiver. The size of the link set $\mathcal{L}$ is denoted as L. In this paper, we only consider the single-channel-per-link scenario. Extension to multiple-channel-per-link scenario is an interesting future work.

We denote the transmission power of a link $l \in \mathcal{L}$ as p_l, the value of which can only be chosen from a discrete power level set $\mathcal{P} = \{P_0, P_1, P_2, \ldots, P_n\}$. For convenience, we set $P_0 \triangleq 0$, and let $P_n \triangleq P_{\max}$ denote the maximum transmission power.

Given $P_{\max}$ and the total number of power levels $n+1$, there are many choices of power level quantizations. Here we consider two types of discrete power level sets [9]:

TABLE 1
Example of Discrete Power Level Sets

Number of Power levels	Exponential Set	Uniform Set
2	$\{0, 1\}$	$\{0, 1\}$
3	$\{0, \frac{1}{2}, 1\}$	$\{0, \frac{1}{2}, 1\}$
4	$\{0, \frac{1}{4}, \frac{1}{2}, 1\}$	$\{0, \frac{1}{3}, \frac{2}{3}, 1\}$
5	$\{0, \frac{1}{8}, \frac{1}{4}, \frac{1}{2}, 1\}$	$\{0, \frac{1}{4}, \frac{1}{2}, \frac{3}{4}, 1\}$
6	$\{0, \frac{1}{16}, \frac{1}{8}, \frac{1}{4}, \frac{1}{2}, 1\}$	$\{0, \frac{1}{5}, \frac{2}{5}, \frac{3}{5}, \frac{4}{5}, 1\}$

exponential power level set and *uniform power level set*. Given the number of power levels $n+1 \geq 2$, exponential power level set is denoted as $\{0\} \cup \{\frac{2^j}{2^{n-1}}, 0 \leq j \leq n-1\}$ and uniform power level set is denoted as $\{\frac{j}{n}, 0 \leq j \leq n\}$. Examples with up to six power levels are shown in Table 1. Here each element in a power level set represents the ratio between the corresponding power level and the maximum transmission power $P_{\max}$. For example, the power level set $\{0, 1/4, 1/2, 1\}$ means that each link can select from four power levels: zero, a quarter, a half, and a full power.

We assume that the channel coherence time is short enough for us to average out the impact of fast fading in our model. In other words, we can focus on the average channel condition (which depends mainly on the path loss) without worrying about the impact of fast fading. The transmission rate of each link $l \in \mathcal{L}$ is denoted as $R_l = f(\text{SINR}_l)$, which is determined by the SINR at its receiver,

$$\text{SINR}_l \triangleq \frac{h_{ll} p_l}{N_0 + \sum_{k \neq l} h_{lk} p_k}, \tag{1}$$

where h_{lk} denotes the channel gain from the link k's transmitter to link l's receiver. According to different SINR levels, links adjust the data rate by choosing different MCSs. When the channel condition significantly improves, a higher order modulation can be chosen to achieve a higher data rate. Thus the data rate can be modeled as the following step function:

$$f(\text{SINR}_l) = \begin{cases} 0, & \text{if } \text{SINR}_l < \gamma_0, \\ r_1, & \text{if } \gamma_0 \leq \text{SINR}_l < \gamma_1, \\ & \vdots \\ r_m, & \text{if } \text{SINR}_l \geq \gamma_m. \end{cases} \tag{2}$$

In Table 2, we show one example of the step function coming from the practical system setting [22]. There are 11 available MCSs. For each MCS, Table 2 lists the corresponding spectrum efficiency and required SINR level.

We assume that once each link decides a power level, it also selects the "best MCS" for the current transmission, which achieves the highest spectrum efficiency (i.e., the largest transmission rate) that can be supported by its current SINR level. This simplifies our description, i.e., we can simply represent a joint power control and MCS adaptation decision by specifying its power level selection.

Now we define the *power configuration* as transmission power vector of all links, i.e., $\boldsymbol{p} \triangleq (p_1, p_2, \ldots, p_L)$. Given a particular power configuration $\boldsymbol{p}$, let $p_l(\boldsymbol{p})$ and $R_{l\boldsymbol{p}}$ denote the power level and rate of link l respectively. We denote $\mathcal{P}$ as the set of all possible power configurations. Our objective

TABLE 2
Example of Modulation-Coding-Schemes (MCSs)

MCS	Spectrum efficiency (bit/s/Hz)	Required SINR (dB)
QPSK 1/2	1.0	6.3
QPSK 5/8	1.25	8.5
QPSK 3/4	1.5	11
QPSK 5/6	1.67	13.8
16QAM 1/2	2.0	11.8
64QAM 1/2	3.0	16
16QAM 3/4	3.0	17
64QAM 5/8	3.75	19.3
64QAM 2/3	4	20.5
64QAM 3/4	4.5	22
64QAM 5/6	5	24.5

is to choose some power configurations from set $\mathcal{P}$, to maximize the total transmission rate of all links. We formulate it as a combinatorial optimization problem, shown as follows:

$$\max_{\boldsymbol{p} \in \mathcal{P}} \sum_{l \in \mathcal{L}} R_{l\boldsymbol{p}}. \tag{3}$$

Such a rate maximization problem is NP-hard [23], which means that there is no efficient algorithm to solve it in a centralized way. Next we will show how we can solve it near-optimally in a distributed way.

3 Algorithm Design and Analysis

We design a distributed approximation algorithm via the Markov approximation framework [24], which is a generalization of distributed MCMC (Markov Chain Monte Carlo) and distributed simulated annealing. There are two key steps for such an approach: First, transform the original combinatorial problem to an equivalent sampling problem with a given probability distribution. Second, sample (or approximately sample) the given probability distribution by constructing a Markov chain distributedly, which has the desirable distribution as its unique stationary distribution.

We denote the set of optimal solutions for problem (3) as $\mathcal{P}^o$, and denote the size of set $\mathcal{P}^o$ as $|\mathcal{P}^o|$. Then we have:

$$\mathcal{P}^o = \arg\max_{\boldsymbol{p} \in \mathcal{P}} \sum_{l \in \mathcal{L}} R_{l\boldsymbol{p}}. \tag{4}$$

We associate each power configuration $\boldsymbol{p} \in \mathcal{P}$ with a probability $\pi_{\boldsymbol{p}}$. Then solving problem (3) is equivalent to sampling the space of power configurations $\mathcal{P}$ from the following general Dirac distribution:

$$\pi^d_{\boldsymbol{p}} = \begin{cases} \frac{1}{|\mathcal{P}^o|}, & \text{if } \boldsymbol{p} \in \mathcal{P}^o, \\ 0, & \text{otherwise.} \end{cases} \tag{5}$$

However, the above general Dirac distribution is hard to obtain, since $\mathcal{P}^o$ is unknown to us. Therefore, we need to sample the space of power configuration $\mathcal{P}$ with a new target distribution, which is more tractable than the general Dirac distribution, and more importantly, satisfies the following two conditions:

- *C1*: it can be obtained without knowing the exact value of $\mathcal{P}^o$.
- *C2*: power configurations in set $\mathcal{P}^o$ have the largest probabilities.

It turns out that the following product-form distribution parameterized by $\sigma > 0$ is a nice choice [24], [25]:

$$\pi^*_{\boldsymbol{p}} = \frac{\exp\left(\frac{1}{\sigma}\sum_{l\in\mathcal{L}} R_{l\boldsymbol{p}}\right)}{\sum_{\boldsymbol{p}'\in\mathcal{P}} \exp\left(\frac{1}{\sigma}\sum_{l\in\mathcal{L}} R_{l\boldsymbol{p}'}\right)}, \forall\, \boldsymbol{p}\in\mathcal{P}. \tag{6}$$

As we will prove later, the advantages of this product-form distribution (6) lie in: 1) it can be obtained by designing a time-reversible Markov chain without knowing the value of $\mathcal{P}^o$, 2) Given a positive constant σ, we can see $\mathcal{P}^o = \arg\max_{\boldsymbol{p}\in\mathcal{P}} \pi^*_{\boldsymbol{p}}$. Thus both conditions *C1* and *C2* are satisfied.

In other words, when we sample the power configuration space $\mathcal{P}$ based on the distribution $\pi^*_{\boldsymbol{p}}$ in (6), we actually solve the problem (3) approximately and obtain a close-to-optimal value. In fact, as $\sigma \to 0$, the product form degrades into the general Dirac distribution. Intuitively, starting from any initial power configuration, the system can find a path to optimal power configurations of the set $\mathcal{P}^o$ by "hopping" across the Markov chain. When the designed Markov chain converges, the system will stay in power configuration set $\mathcal{P}^o$ most of the time. In this sense, we approximately solve the original rate maximization problem.

Now we show how to design a time-reversible power-hopping Markov chain, with a state space being the set of all feasible power configurations $\mathcal{P}$ and a stationary distribution being the product-form distribution given by (6). Distributed MCMC is typically considered under continuous-time (or asynchronous) setting as in [24], [25], which is also our target scenario. There are two degrees of freedom in designing a time-reversible power-hopping Markov chain in a distributed manner:

- *The state space structure:* The state space of the Markov chain should be connected, such that any two states are reachable from each other. To enable distributed implementations, we design the Markov chain state space such that a direct transition from one state to another state corresponds to one and only one link (out of L links) adjusting its transmission power levels.
- *Direct transition rates:* For any two states $\boldsymbol{p}, \boldsymbol{p}' \in \mathcal{P}$ with direct transitions (on both directions), the corresponding transition rates between them should satisfy the detailed balance equation for time-reversibility: $\pi_{\boldsymbol{p}} \cdot q_{\boldsymbol{p},\boldsymbol{p}'} = \pi_{\boldsymbol{p}'} \cdot q_{\boldsymbol{p}',\boldsymbol{p}}$, where $q_{\boldsymbol{p},\boldsymbol{p}'}$ is the transition rate from state $\boldsymbol{p}$ to state $\boldsymbol{p}'$. To enable distributed implementations, computation of transition rates should involve only local network information.

With the above guideline, we design the Markov chain as follows:

- Each power configuration $\boldsymbol{p} \in \mathcal{P}$ is a state of the Markov chain. There are direct transitions between two states $\boldsymbol{p}, \boldsymbol{p}' \in \mathcal{P}$ if and only if $\boldsymbol{p}$ and $\boldsymbol{p}'$ differ in only one link's power level.
- For any two states $\boldsymbol{p}, \boldsymbol{p}'$ that have direct transitions, we have two options for the corresponding transition rates between them:
  - Option 1

$$q_{\boldsymbol{p},\boldsymbol{p}'} = \frac{C}{\exp\left(\frac{1}{\sigma}\left(\sum_{l\in\mathcal{L}} R_{l\boldsymbol{p}} - \sum_{l\in\mathcal{L}} R_{l\boldsymbol{p}'}\right)\right) + 1}, \tag{7}$$

$$q_{\boldsymbol{p}',\boldsymbol{p}} = \frac{C}{\exp\left(\frac{1}{\sigma}\left(\sum_{l\in\mathcal{L}} R_{l\boldsymbol{p}'} - \sum_{l\in\mathcal{L}} R_{l\boldsymbol{p}}\right)\right) + 1}, \tag{8}$$

  where C is an arbitrary positive constant.
  - Option 2

$$q_{\boldsymbol{p},\boldsymbol{p}'} = \frac{C}{\max\left(\exp\left(\frac{1}{\sigma}\left(\sum_{l\in\mathcal{L}} R_{l\boldsymbol{p}} - \sum_{l\in\mathcal{L}} R_{l\boldsymbol{p}'}\right)\right), 1\right)}, \tag{9}$$

$$q_{\boldsymbol{p}',\boldsymbol{p}} = \frac{C}{\max\left(\exp\left(\frac{1}{\sigma}\left(\sum_{l\in\mathcal{L}} R_{l\boldsymbol{p}'} - \sum_{l\in\mathcal{L}} R_{l\boldsymbol{p}}\right)\right), 1\right)}, \tag{10}$$

  where C is an arbitrary positive constant.

We choose the above transition rates because of the following consideration. Given any power configuration $\boldsymbol{p}$, the total data rate $\sum_{l\in\mathcal{L}} R_{l\boldsymbol{p}}$ is hard to compute locally by any particular link since it requires global channel information. Thus we consider the difference between $\sum_{l\in\mathcal{L}} R_{l\boldsymbol{p}}$ and $\sum_{l\in\mathcal{L}} R_{l\boldsymbol{p}'}$, which is easy to obtain locally. For each link $l \in \mathcal{L}$, we define the rate change of link l as

$$\Delta R_l(\boldsymbol{p}, \boldsymbol{p}') = R_{l\boldsymbol{p}} - R_{l\boldsymbol{p}'}.$$

Then we know

$$\sum_{l\in\mathcal{L}} R_{l\boldsymbol{p}} - \sum_{l\in\mathcal{L}} R_{l\boldsymbol{p}'} = \sum_{l\in\mathcal{L}} \Delta R_l(\boldsymbol{p}, \boldsymbol{p}').$$

Since direct state transition from $\boldsymbol{p}$ to $\boldsymbol{p}'$ corresponds to one and only one link adjusting its transmission power level. For convenience, we denote this link as $\bar{l}$, which change its power level from $p_{\bar{l}}(\boldsymbol{p})$ to $p_{\bar{l}}(\boldsymbol{p}')$. Such a change affects the SINRs of *all* links. However, it will only change rates of *some* links, due to the stepwise mapping between SINR and transmission rates in (2). We denote $\tilde{\mathcal{L}}$ as the set of links whose rate changes because of link $\bar{l}$'s transmission power change, i.e., $\Delta R_l(\boldsymbol{p}, \boldsymbol{p}') \neq 0, \forall l \in \tilde{\mathcal{L}}$. Therefore,

$$\Delta R_l(\boldsymbol{p}, \boldsymbol{p}') = 0, \forall l \in \mathcal{L} \setminus \tilde{\mathcal{L}},$$
$$\sum_{l\in\mathcal{L}} R_{l\boldsymbol{p}} - \sum_{l\in\mathcal{L}} R_{l\boldsymbol{p}'} = \sum_{l\in\tilde{\mathcal{L}}} \Delta R_l(\boldsymbol{p}, \boldsymbol{p}').$$

According to (1) and assuming the channel gain is dominated by the distance-based path loss component, $\bar{l}$'s neighboring links are more likely to be affected than links far away from link $\bar{l}$. Thus links in the set $\tilde{\mathcal{L}}$ are more likely to be the near neighbors of link $\bar{l}$, hence we regard set $\tilde{\mathcal{L}}$ as a "semi-local" set of link $\bar{l}$. In this sense, the difference between $\sum_{l\in\mathcal{L}} R_{l\boldsymbol{p}}$ and $\sum_{l\in\mathcal{L}} R_{l\boldsymbol{p}'}$, i.e., $\sum_{l\in\mathcal{L}} R_{l\boldsymbol{p}} - \sum_{l\in\mathcal{L}} R_{l\boldsymbol{p}'}$, is a "semi-local" information and can be obtained through distributed implementations.

We design the following ARM algorithm to construct the designed power-hopping Markov chain. We emphasize that the executions of ARM by different links are asynchronous. In ARM, for each link $l \in \mathcal{L}$, there are three phases

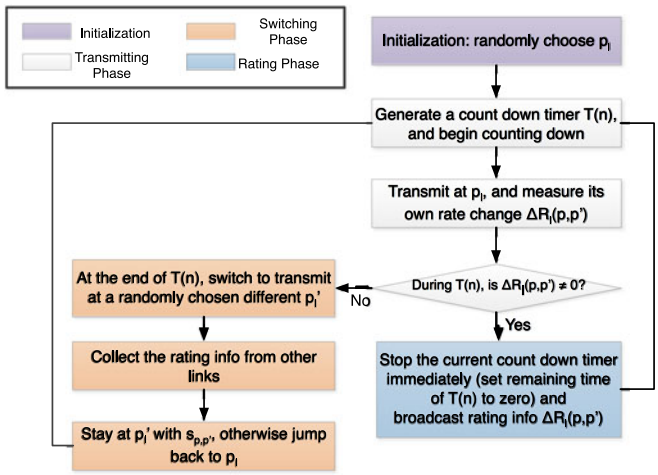

Fig. 1. Flowchart of ARM.

after the initialization of power level setting: transmitting phase, rating phase, and switching phase.

- *Transmitting phase*: At the beginning of this phase, each link $l \in \mathcal{L}$ starts a random counter-down timer with a countdown time $T(n)$. The value of $T(n)$ is generated based on an exponential distribution with a mean $\frac{1}{nC}$, where $n+1$ is the number of discrete power levels and C is a system parameter chosen according to different system requirements. Within the countdown time $T(n)$, link l transmits at its current power level p_l. In the meantime, link l also observes whether his own SINR experiences a change (due to some other link changing his transmission power) such that there is a need to change its choice of rate according to (2), link l immediately terminates the transmitting phase and begins the rating phase. On the other hand, if link l does not observe any rate change during time $T(n)$, it will begin the switching phase when the count-down timer reaches zero.
- *Rating phase*: At the beginning of this phase, link l will stop its current count-down timer and broadcast its rate change information. A small number of bits are enough to represent the rating information, because there are only a limited choices of available data rates. This ensures the low communication overhead during this phase. After this, link l will restart the transmitting phase.
- *Switching phase:*[1] At the beginning of this phase, link l transmits at a randomly chosen new power level $p_l(\boldsymbol{p}')$. Then it will collect the rate change information those links who are triggered to enter the rating phase. Next, it will set its current transmission power level to be $p_l(\boldsymbol{p}')$ with probability $s_{\boldsymbol{p},\boldsymbol{p}'} = \frac{1}{\exp\left(\frac{1}{\sigma}\left(\sum_{l' \neq l} \Delta R_{l'}(\boldsymbol{p},\boldsymbol{p}')\right)\right)+1}$ under the design of Option 1, and with probability $s_{\boldsymbol{p},\boldsymbol{p}'} = \frac{1}{\max\left(\exp\left(\frac{1}{\sigma}\left(\sum_{l' \neq l} \Delta R_{l'}(\boldsymbol{p},\boldsymbol{p}')\right)\right),1\right)}$ under the design of Option 2, or it will switch its transmission power level back to p_l with probability $1 - s_{\boldsymbol{p},\boldsymbol{p}'}$. Then link l will restart the transmitting phase.

We summarize the algorithm by a form of flowchart in Fig. 1.

Remarks.

- ARM does not require synchronization or explicit coordination among links, and the only communication overhead is the simple rate change information, which makes ARM suitable for parallel and distributed implementation in wireless ad hoc networks.
- To implement ARM in the LTE system, we need to exchange rate change informations among links with low signaling overhead. There are two methods proposed in [26]. One is the over-the-air method, using the existing CQI (channel quality indicator) channel in LTE with extra rate change information. More specifically, Each User feedbacks the CQI information and extra information about the rate changes directly to the base station. The other is the backhaul method, using the existing low-bit-rate X2 channel in LTE to exchange rate change information among transmitters and base-stations. Since the number of possible values of rate changes is low due to limited power levels and MCSs, the overall signaling (communication) overhead is low no matter which method to use.
- Connection between rating phase and online rating systems: if a link achieves a lower data rate due to the increase of power and interference from its neighbor, then it will feedback a negative rate difference to such neighbor. Conversely, if it achieves a higher rate due to its neighbor's power decrease, then it will feedback a positive rate difference to such neighbor. This process is just like the rating system in Amazon, where one customer rates five stars to a good book, or one star to a bad one. In addition, since there are just a limited number of possible rates in the real system, there are just a limited possibilities of rate changes for each link, which can be mapped to a rating system of finite choices.
- It is possible that change of power by one link can have long-range effects, i.e., not "semi-local" any more. When this happens, the local estimation method described in Section 3.1 will lead to inaccurate rating information. However, as we will show in Section 3.1, our algorithm is robust to such inaccuracy. In fact, we can have a controlled and bounded performance gap, which is the price we need to pay for the desire of distributed algorithm design and scalability.

We can show the following result:

Proposition 1. *The ARM algorithms with two variants (option 1 (7) and option 2 (9)) construct time-reversible Markov chains with the desired stationary distribution in (6).*

Proof. Here we only show the case for ARM with option 1 (7). The proof of the other case for ARM with option 2 (9) is similar and we omit the details due to the space limit.

1. Other links change their rates at the end of the switching phase of link l. Ideally, the switching phase happens instantaneously and there are no loss of data. In practice, the duration of the switching phase is non-zero, there are data losses during that period. However, as we show in Section 3.1, we can regard such loss as the inaccuracy of data rates and our algorithm is robust to such inaccuracy.

For any two states that do not have direct transitions, the corresponding power configurations differ in at least two link's power levels. We can always find a finite path to connect these two states by adjusting the power level of only one link's transmitter at each transition. Since these two state are arbitrary, the whole state space is connected, resulting an irreducible Markov chain. Furthermore, its state space is finite, resulting an ergodic Markov chain with a unique stationary distribution. We now show that the stationary distribution is indeed (6).

Since each link counts down with a rate $n \times C$, given the current state $\boldsymbol{p}$, the process leaves state $\boldsymbol{p}$ with a rate $n \times C \times L$. With probability $\frac{1}{n \times L}$, the process jumps to an adjacent state $\mathbf{p}'$ and stays in this new state with probability $\frac{1}{\exp\left(\frac{1}{\sigma}\left(\sum_{l' \neq l} \Delta R_{l'}(\boldsymbol{p},\boldsymbol{p}')\right)\right)+1}$. Then we can calculate the transition rate from state p to state p' as follows:

$$\frac{1}{n\,L} \times n \times C \times L \times \frac{1}{\exp\left(\frac{1}{\sigma}\left(\sum_{l' \neq l} \Delta R_{l'}(\boldsymbol{p},\boldsymbol{p}')\right)\right)+1} = \frac{C}{\exp\left(\frac{1}{\sigma}\left(\sum_{l \in \mathcal{L}} R_{l\boldsymbol{p}} - \sum_{l \in \mathcal{L}} R_{l\boldsymbol{p}'}\right)\right)+1}. \tag{11}$$

With (6), we see that $\pi_{\boldsymbol{p}}\, q_{\boldsymbol{p},\boldsymbol{p}'} = \pi_{\boldsymbol{p}'}\, q_{\boldsymbol{p}',\boldsymbol{p}}$, i.e., the detailed balance equation holds between any two adjacent states. Thus the constructed Markov chain is time-reversible and its stationary distribution is indeed (6) according to [27]. □

We can understand ARM in an intuitive way. In this algorithm, "good states" (i.e., those having high total data rates) or "bad states" (i.e., those having a low total data rates) are voted through links' rating information. With carefully designed transition rates, ARM ensures that the system is capable of jumping into "good states" with high probabilities, but also is capable of exploiting "bad states" occasionally so as to avoid being trapped in a local optimal state (where the level of exploitation is parameterized by the approximation factor σ). As a result, the system stays in "good states" with high probabilities, and eventually stays in the "best states" with the highest probabilities.

Next we study two issues related to the practical implementation of ARM: robustness and convergence time.

3.1 Robustness of ARM

In practice, one link may obtain inaccurate values of rating information (i.e., $\Delta R_l(\boldsymbol{p},\boldsymbol{p}')$) from other links. The inaccuracy comes from two sources of perturbation:

- *Transmission errors or losses*: Erroneous and lossy wireless transmissions of rating information lead to inaccurate and out of date rating messages.
- *Local estimation*: To further reduce the complexity of ARM and facilitate the distributed implementation, each link may collect the rating information only from a small set of neighboring links. Such a local estimation leads to inaccurate total rating information.

Consequently, with perturbations, we obtain a new perturbed Markov chain: whose state space is still $\mathcal{P}$, but whose transition rates are perturbed versions of options 1 and 2. This perturbed Markov chain may *not* converge to the desired stationary distribution $\pi^*_{\boldsymbol{p}}$ (6), resulting in another stationary distribution and a performance gap. To characterize such a gap, we adopt the following quantization error model similar to those proposed in [28]. In this model, for each state $\boldsymbol{p} \in \mathcal{P}$ and each link $l \in \mathcal{L}$ with data rate $R_{l\boldsymbol{p}}$, we denote its corresponding perturbation error as $\Delta_{l,\boldsymbol{p}}$. We assume it is discrete, symmetric and upper bounded, i.e., $\mathbb{E}(\Delta_{l,\boldsymbol{p}}) = 0$ and $|\Delta_{l,\boldsymbol{p}}| \leq \Delta_{\max}$, where $\Delta_{\max}$ is a positive constant. Therefore, for each state $\boldsymbol{p} \in \mathcal{P}$, the aggregated data rates are perturbed as $\sum_{l \in \mathcal{L}}(R_{l\boldsymbol{p}} + \Delta_{l,\boldsymbol{p}})$.

Let $\phi_{\max}$ denote the aggregate rates of all links under the optimal power configuration, i.e., $\phi_{\max} = \sum_{l \in \mathcal{L}} R_{l\boldsymbol{p}}, \forall \boldsymbol{p} \in \mathcal{P}^o$. Let ϕ_a denote the expected aggregate rates of all links with the power-hopping Markov chain, i.e., $\phi_a = \sum_{\boldsymbol{p} \in \mathcal{P}} \pi^*_{\boldsymbol{p}} \cdot (\sum_{l \in \mathcal{L}} R_{l\boldsymbol{p}})$. Let ϕ_e denote the expected aggregate rates of all links with the perturbed power-hopping Markov chain, i.e., $\phi_e = \sum_{\boldsymbol{p} \in \mathcal{P}} \pi^e_{\boldsymbol{p}} \cdot (\sum_{l \in \mathcal{L}} R_{l\boldsymbol{p}})$, where $\pi^e_{\boldsymbol{p}}$ is the stationary distribution of the perturbed Markov chain. By perturbation analysis developed in [28], we have the same following result for ARM with either option 1 or option 2:

Theorem 1. *(a) The stationary distribution of the perturbed power-hopping Markov chain is*

$$\pi^e_{\boldsymbol{p}} = \frac{\beta_{\boldsymbol{p}} \cdot \exp\left(\frac{1}{\sigma}\sum_{l \in \mathcal{L}} R_{l\boldsymbol{p}}\right)}{\sum_{\boldsymbol{p}' \in \mathcal{P}} \beta_{\boldsymbol{p}'} \cdot \exp\left(\frac{1}{\sigma}\sum_{l \in \mathcal{L}} R_{l\boldsymbol{p}'}\right)}, \forall\, \boldsymbol{p} \in \mathcal{P}, \tag{12}$$

where $\beta_{\boldsymbol{p}} = \mathbb{E}\left[\exp\left(\frac{1}{\sigma} \cdot \left(\sum_{l \in \mathcal{L}} \Delta_{l,\boldsymbol{p}}\right)\right)\right], \forall\, \boldsymbol{p} \in \mathcal{P}$.

(b) Bounds on the optimality gap for both power-hopping Markov chain and its perturbed counterpart are:

$$0 \leq \phi_{\max} - \phi_a \leq L \cdot \sigma \cdot \log(n+1) - \sigma \cdot \log|\mathcal{P}^o|, \tag{13}$$

$$0 \leq \phi_{\max} - \phi_e \leq L \cdot \sigma \cdot \log(n+1) - \sigma \cdot \log|\mathcal{P}^o| + L \cdot \Delta_{\max}. \tag{14}$$

Proof. Here we only show the case for ARM with option 1 in (7). The proof of the other case for ARM with option 2 in (9) is similar and we omit the details due to the space limit. The proof for part (a) adopts similar technique in [28] and is omitted to save space. Now we focus on the proof for part (b).

First we show the inequalities in (13). By [24] we know that probability distribution $\pi^*_{\boldsymbol{p}}$ in (6) is the optimal solution to the following maximization problem:

$$\max \sum_{\boldsymbol{p} \in \mathcal{P}} \pi_{\boldsymbol{p}} \cdot \left(\sum_{l \in \mathcal{L}} R_{l\boldsymbol{p}}\right) - \sigma \cdot \sum_{\boldsymbol{p} \in \mathcal{P}} \pi_{\boldsymbol{p}} \log \pi_{\boldsymbol{p}}, \tag{15}$$

$$\text{s.t.} \sum_{\boldsymbol{p} \in \mathcal{P}} \pi_{\boldsymbol{p}} = 1, \tag{16}$$

$$\pi_{\boldsymbol{p}} \geq 0, \forall \boldsymbol{p} \in \mathcal{P}. \tag{17}$$

Since the general Dirac distribution $\pi^d_{\boldsymbol{p}}$ in (5) is a feasible solution for the above maximization problem, we have

$$\sum_{\boldsymbol{p} \in \mathcal{P}} \pi^*_{\boldsymbol{p}} \cdot \left(\sum_{l \in \mathcal{L}} R_{l\boldsymbol{p}}\right) - \sigma \cdot \sum_{\boldsymbol{p} \in \mathcal{P}} \pi^*_{\boldsymbol{p}} \log \pi^*_{\boldsymbol{p}}, \tag{18}$$

$$\geq \sum_{\boldsymbol{p}\in\mathcal{P}} \pi^d_{\boldsymbol{p}} \cdot \left(\sum_{l\in\mathcal{L}} R_{l\boldsymbol{p}}\right) - \sigma \cdot \sum_{\boldsymbol{p}\in\mathcal{P}} \pi^d_{\boldsymbol{p}} \log \pi^d_{\boldsymbol{p}}, \tag{19}$$

$$= \phi_{\max} + \sigma \cdot \log |\mathcal{P}^o|. \tag{20}$$

By Jensen's inequality, we know that

$$-\sum_{\boldsymbol{p}\in\mathcal{P}} \pi^*_{\boldsymbol{p}} \log \pi^*_{\boldsymbol{p}} = \sum_{\boldsymbol{p}\in\mathcal{P}} \pi^*_{\boldsymbol{p}} \log \frac{1}{\pi^*_{\boldsymbol{p}}}, \tag{21}$$

$$\leq \log\left(\sum_{\boldsymbol{p}\in\mathcal{P}} \pi^*_{\boldsymbol{p}} \cdot \frac{1}{\pi^*_{\boldsymbol{p}}}\right) = \log|\mathcal{P}| = L \cdot \log(n+1). \tag{22}$$

Combining (20) and (22), we have

$$\phi_a \triangleq \sum_{\boldsymbol{p}\in\mathcal{P}} \pi^*_{\boldsymbol{p}} \cdot \left(\sum_{l\in\mathcal{L}} R_{l\boldsymbol{p}}\right), \tag{23}$$

$$\geq \phi_{\max} + \sigma \cdot \log|\mathcal{P}^o| - L \cdot \log(n+1). \tag{24}$$

On the other hand, since $\phi_a \leq \phi_{\max}$, we have

$$0 \leq \phi_{\max} - \phi_a \leq L \cdot \sigma \cdot \log(n+1) - \sigma \cdot \log|\mathcal{P}^o|. \tag{25}$$

Next we show the inequalities in (14). By (12) we know the perturbed stationary distribution is

$$\pi^e_{\boldsymbol{p}} = \frac{\beta_{\boldsymbol{p}} \cdot \exp\left(\frac{1}{\sigma}\sum_{l\in\mathcal{L}} R_{l\boldsymbol{p}}\right)}{\sum_{\boldsymbol{p}'\in\mathcal{P}} \beta_{\boldsymbol{p}'} \cdot \exp\left(\frac{1}{\sigma}\sum_{l\in\mathcal{L}} R_{l\boldsymbol{p}'}\right)}, \tag{26}$$

$$= \frac{\exp\left(\frac{1}{\sigma}\left(\sigma \cdot \log \beta_{\boldsymbol{p}} + \sum_{l\in\mathcal{L}} R_{l\boldsymbol{p}}\right)\right)}{\sum_{\boldsymbol{p}'\in\mathcal{P}} \exp\left(\frac{1}{\sigma}\left(\sigma \cdot \log \beta_{\boldsymbol{p}'} + \sum_{l\in\mathcal{L}} R_{l\boldsymbol{p}'}\right)\right)}, \forall\, \boldsymbol{p} \in \mathcal{P}. \tag{27}$$

Therefore, probability distribution $\pi^e_{\boldsymbol{p}}$ can be viewed as the optimal solution to the following maximization problem:

$$\begin{aligned} &\max \sum_{\boldsymbol{p}\in\mathcal{P}} \pi_{\boldsymbol{p}} \cdot \left(\sigma \cdot \log \beta_{\boldsymbol{p}} + \sum_{l\in\mathcal{L}} R_{l\boldsymbol{p}}\right) - \sigma \cdot \sum_{\boldsymbol{p}\in\mathcal{P}} \pi_{\boldsymbol{p}} \log \pi_{\boldsymbol{p}} \\ &\text{s.t.} \sum_{\boldsymbol{p}\in\mathcal{P}} \pi_{\boldsymbol{p}} = 1, \end{aligned} \tag{28}$$

$$\pi_{\boldsymbol{p}} \geq 0, \forall \boldsymbol{p} \in \mathcal{P}. \tag{29}$$

By (25), we have

$$\begin{aligned} &\max_{\boldsymbol{p}\in\mathcal{P}} \left(\sigma \cdot \log \beta_{\boldsymbol{p}} + \sum_{l\in\mathcal{L}} R_{l\boldsymbol{p}}\right) - \sum_{\boldsymbol{p}\in\mathcal{P}} \pi^e_{\boldsymbol{p}} \cdot \left(\sigma \cdot \log \beta_{\boldsymbol{p}} + \sum_{l\in\mathcal{L}} R_{l\boldsymbol{p}}\right), \\ &\leq L \cdot \sigma \cdot \log(n+1) - \sigma \cdot \log|\mathcal{P}^o|. \end{aligned} \tag{30}$$

For any $\boldsymbol{p} \in \mathcal{P}$, we have

$$\beta_{\boldsymbol{p}} = \mathbb{E}\left[\exp\left(\frac{1}{\sigma} \cdot \left(\sum_{l\in\mathcal{L}} \Delta_{l,\boldsymbol{p}}\right)\right)\right], \tag{31}$$

$$\leq \exp\left(\frac{L}{\sigma} \cdot \Delta_{\max}\right). \tag{32}$$

Therefore we have

$$\sigma \cdot \log \beta_{\boldsymbol{p}} \leq L \cdot \Delta_{\max}, \forall \boldsymbol{p} \in \mathcal{P}. \tag{33}$$

Note that

$$\phi_e \triangleq \sum_{\boldsymbol{p}\in\mathcal{P}} \pi^e_{\boldsymbol{p}} \cdot \left(\sum_{l\in L} R_{l\boldsymbol{p}}\right). \tag{34}$$

Then we have

$$\begin{aligned} &\sum_{\boldsymbol{p}\in\mathcal{P}} \pi^e_{\boldsymbol{p}} \cdot \left(\sigma \cdot \log \beta_{\boldsymbol{p}} + \sum_{l\in\mathcal{L}} R_{l\boldsymbol{p}}\right), \\ &\leq \sum_{\boldsymbol{p}\in\mathcal{P}} \pi^e_{\boldsymbol{p}} \cdot L \cdot \Delta_{\max} + \phi_e, \end{aligned} \tag{35}$$

$$= L \cdot \Delta_{\max} + \phi_e. \tag{36}$$

Note that for any $l \in \mathcal{L}$ and $\boldsymbol{p} \in \mathcal{P}$, $\mathbb{E}(\Delta_{l,\boldsymbol{p}}) = 0$. By Jensen's inequality, we know that for any $\boldsymbol{p} \in \mathcal{P}$, we have

$$\beta_{\boldsymbol{p}} = \mathbb{E}\left[\exp\left(\frac{1}{\sigma} \cdot \left(\sum_{l\in\mathcal{L}} \Delta_{l,\boldsymbol{p}}\right)\right)\right], \tag{37}$$

$$\geq \exp\left(\mathbb{E}\left[\frac{1}{\sigma} \cdot \left(\sum_{l\in\mathcal{L}} \Delta_{l,\boldsymbol{p}}\right)\right]\right), \tag{38}$$

$$= \exp\left(\frac{1}{\sigma} \cdot \left(\sum_{l\in\mathcal{L}} \mathbb{E}\left[\Delta_{l,\boldsymbol{p}}\right]\right)\right), \tag{39}$$

$$= 1. \tag{40}$$

Therefore, we have

$$\sigma \cdot \log \beta_{\boldsymbol{p}} \geq 0, \forall \boldsymbol{p} \in \mathcal{P}, \tag{41}$$

and

$$\phi_{\max} = \max_{\boldsymbol{p}\in\mathcal{P}} \sum_{l\in\mathcal{L}} R_{l\boldsymbol{p}}, \tag{42}$$

$$\leq \max_{\boldsymbol{p}\in\mathcal{P}} \left(\sigma \cdot \log \beta_{\boldsymbol{p}} + \sum_{l\in\mathcal{L}} R_{l\boldsymbol{p}}\right). \tag{43}$$

By combining (30), (36) and (43), we have

$$0 \leq \phi_{\max} - \phi_e \leq L \cdot \sigma \cdot \log(n+1) - \sigma \cdot \log|\mathcal{P}^o| + L \cdot \Delta_{\max}. \tag{44}$$

□

Remarks.

- The upper bounds on the optimality gap for both the power-hopping Markov chain in (13) and its perturbed counterpart in (14) increase linearly with the number of links L and the approximation factor σ, increase log-linearly with the number of discrete power levels $n+1$, and decrease log-linearly with the number of optimal power configurations $|\mathcal{P}^o|$.
- The upper bound on the optimality gap of perturbed Markov chain in (14) is quite general, as it is

independent of the distribution of perturbation errors for each link $\Delta_{l,\boldsymbol{p}}$.

- For ARM with option 1 in (7) and option 2 in (9), the corresponding optimality gaps are the same, which means that given sufficiently long time, the performances of ARM with option 1 and option 2 are the same. However, if the running time is limited, the corresponding performance and robustness are different. We will demonstrate this in Sections 3.2 and 4.
- When the optimal power configuration is unique, i.e., $|\mathcal{P}^o| = 1$, the upper bounds on the optimality gap for both the power-hopping Markov chain in (13) and its perturbed counterpart in (14) are independent of the size of the optimal power configuration set $|\mathcal{P}^o|$.

3.2 Convergence Time of ARM

Now we study the mixing time (convergence time) of the designed Markov chains with both option 1 (7) and option 2 (9). First, we introduce the definition of *total variation distance* [29] between any two probability distributions π and π' over state space $\mathcal{P}$ as follows:

$$||\pi - \pi'||_{TV} \triangleq \frac{1}{2}\sum_{\boldsymbol{p}\in\mathcal{P}} |\pi_{\boldsymbol{p}} - \pi'_{\boldsymbol{p}}|. \tag{45}$$

Now let $\pi_t(\boldsymbol{p})$ denote the probability distribution of all states in $\mathcal{P}$ at time t, given that the initial state is $\boldsymbol{p}$ and the system evolves according to ARM. Then the *mixing time* of the designed Markov chain [29] is parameterized by an error tolerance parameter ϵ as follows:

$$t_{\text{mix}}(\epsilon) \triangleq \inf\left\{t \geq 0 : \max_{\boldsymbol{p}\in\mathcal{P}} ||\pi_t(\boldsymbol{p}) - \pi^*||_{TV} \leq \epsilon\right\}, \tag{46}$$

where π^* is the stationary distribution shown in (6).

We denote two threshold values $\sigma^1_{th} = \frac{L\cdot r_m}{\ln(1+\frac{1+1/n}{L-1})}$ and $\sigma^2_{th} = \frac{L\cdot r_m}{\ln(1+\frac{L+1/n}{L-1})}$. We also use $\sim$ to represent the relationship of the same order of magnitude. Then we have the following results on the upper bound of the convergence time (mixing time):

Theorem 2. *For the designed Markov chain with option 1 (7) (option 2 (9)) :*

- *If $\sigma > \sigma^1_{th}$ ($\sigma > \sigma^2_{th}$), then the upper bound of mixing time $t_{\text{mix}}(\epsilon)$ is $\sim O\big(\exp(\frac{1}{\sigma})\cdot\ln\frac{L}{\epsilon}\big)$.*
- *If $0 < \sigma \leq \sigma^1_{th}$ ($0 < \sigma \leq \sigma^2_{th}$), then the upper bound of mixing time $t_{\text{mix}}(\epsilon)$ is $\sim \Omega\big(\exp\big(\frac{L}{\sigma} + \ln\ln\frac{1}{\epsilon}\big)\big)$.*

The proof is long and we put it in Section 5. This proof adopts spectral analysis method [29] to obtain both a lower bound and an upper bound of t_{mix} for general values of σ. It also adopts path coupling method [29] to obtain a tight upper bound of t_{mix} for some values of σ.

When σ is a given parameter, we consider the scaling of the optimality gap and mixing time with the network size L. We observe the following trade-off between the optimality gap (Theorem 1) and its mixing time (Theorem 2):

- As $\sigma \to 0$, the optimality gap approaches zero while the upper bound of its mixing time scales with $\Omega(\exp(L))$ and approaches infinity (slow-mixing).

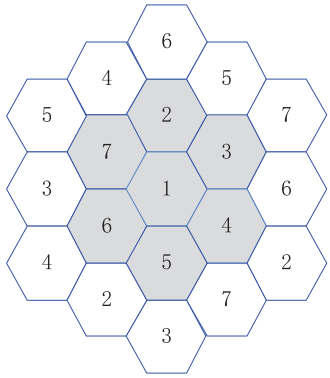

Fig. 2. Seven-cell network with corresponding wrap around: the gray cells are the network we considered, and the white cells denote the wrap-around mappings.

- As $\sigma \to \infty$, the optimality gap approaches infinity while the bound of its mixing time scales with $O(\ln(L))$ and remains limited (fast-mixing).

These are theoretical results from the worst-case analysis. However, in practice, even small values of σ can lead to fast mixing. In fact, simulations in next section show that ARM converges very fast for small values of σ. What is more, since $L > 1$ in general, $\sigma^1_{th} > \sigma^2_{th}$, which means the Markov chain with option 2 usually converges faster than the Markov chain with option 1. In the next section we will show the simulation results to validate this analytical result.

4 Performance Evaluation

4.1 Practical Simulation Setting

For notation simplicity in the whole simulation section, we let ARM1 denote the ARM algorithm with option 1 (7) and ARM 2 denote the ARM algorithm with option 2 (9).

In this simulation, we first focus on a downlink transmission scenario of seven hexagon cells, shown in Fig. 2, where small cells (i.e., the gray cells in Fig. 2) are densely deployed to cover entire area. The border effect is taken care by the wrap-around technique[2] [22]

The main system parameters of simulations are summarized in Table 3, based on the current standardizations of practical cellular system [9]. There are 11 MCSs available for each cell in our simulation, and the spectrum efficiency of each MCS and its required SINR level have been listed in Table 2. We also consider both the exponential power level set and the uniform power level set, where the maximum number of power level sets is five and a full power is 20 dBm.

In the current commercial system, a cell usually has multiple channels to support multiple users, and the cell local scheduler (e.g., the proportional fairness scheduler used in most cellular system) will schedule at most one user for each channel to avoid intra-cell interference. To simplify the simulation, we only simulate the case where each cell has only one channel. The performance of the multiple-channel case can be computed by the proper multiplication of the performance of

2. The wrap-around is commonly used in practical system simulation, where the simulated network is visualized as a torus with edges warping around to the opposite edges, so that each cell has a complete set of interfering cells. The white cells in Fig. 2 denote the wrap-around mappings of the considered network.

TABLE 3
System Parameters

Number of small cells	7
Maximum transmission power of each cell	20 dBm
Radius of each cell	20 m
Noise power spectrum density	-174 dB/Hz
Bandwidth	10 M
Pathloss	$20 \log_{10}(d) + 38.46$ dB

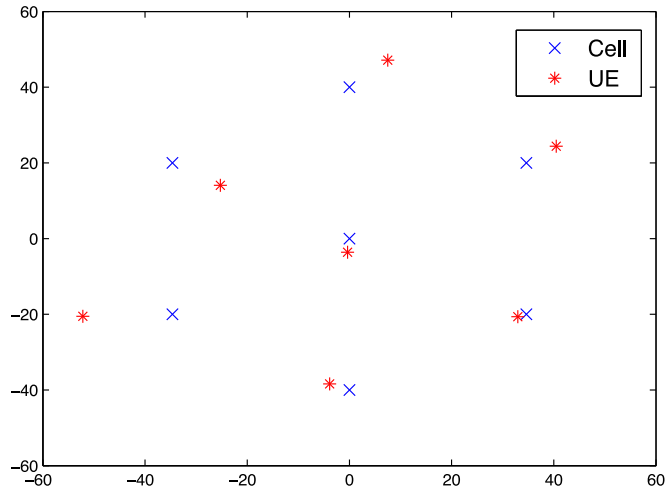

Fig. 3. User position in one experiment (UE stands for user equipment or simply user).

the single channel case, assuming an ideal channel allocation algorithm.[3] Thus in each experiment of the simulation, we randomly pick one user (i.e., mobile device) in each cell, which represents the link chosen by each cell's local scheduler. Each cell runs ARM independently to determine the transmission power and MCS of its user. We run ARM with different values of approximation factor σ and different power level sets, and compare its performances with the optimal solutions generated by exhaustive search. Since performances of ARM1 and ARM2 are very close, here we only provide results of ARM1 for the seven-cell network. In Section 4.4, we will compare the performance of these algorithms in the context of a 61-cell network.

4.2 Impacts of Approximation Factor σ

To investigate the impacts of approximation factor σ, we adopt the following setting: the power level set is $[0, \frac{1}{2}, 1]$, the mean time $1/C$ is 1 unit time, and the maximum number of transitions is chosen to be 10^5. For each experiment, we randomly generate the user positions, with Fig. 3 illustrating one typical example. Fig. 4 shows the convergence of ARM1 under the topology of Fig. 3, with $\sigma = 0.05$. In particular, ARM1 converges reasonably fast, and with 5,000 transitions (which takes around half a second on a standard PC) the performance gap between the achievable value (i.e., 10.9871 bit/s/Hz) and the optimal value (i.e., 11 bit/s/Hz computed through exhaustive search) is less than 0.1 percent .

3. The more detailed modeling of the joint intra-cell channel scheduling and inter-cell discrete power control will be subject to future studies.

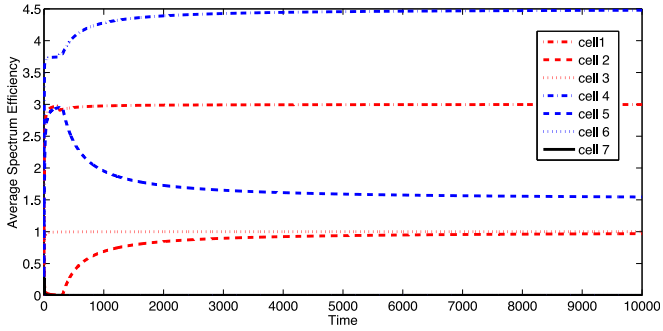

Fig. 4. Average spectrum efficiency in one experiment with $\sigma = 0.05$.

TABLE 4
Average Performance of 1,000 Experiments for ARM1

σ	1	0.5	0.2	0.1	0.05
ES			10.3755		
ARM	8.2202	9.2148	10.1230	10.3118	10.3567
Performance Gap	23%	12%	2.7%	0.7%	0.2%

TABLE 5
Performance Comparison for Exponential Power Level Sets

Number of Power Levels	2	3	4	5
ES (bit/s/Hz)	9.9337	10.3755	10.4713	10.4808
ES Improvement (bit/s/Hz)	–	0.4418	0.0958	0.0095
Performance Ratio	94.78%	98.90%	99.91%	100%
ARM (bit/s/Hz)	9.9241	10.3567	10.4555	10.4593
ARM Improvement (bit/s/Hz)	–	0.4326	0.0988	0.0038
Performance Ratio	94.88%	99.02%	99.96%	100%
Performance Gap	0.1%	0.18%	0.15%	0.21%

We run 1,000 experiments and records the average sum spectrum efficiencies of exhaustive search (ES) and ARM1 (after 10^5 transitions), respectively. Table 4 summarizes the results, which show that a smaller value of σ leads to a higher spectrum efficiency and a smaller performance gap with the optimal one. This result is consistent with the result in Theorem 1.

4.3 Impacts of Power Levels

Continuous power levels can be regarded as the limiting case of discrete power levels, where the number of power levels becomes large enough. Given a fixed power range (e.g., minimum and maximum), more power levels will provide more flexibility to power control and thus improve the performance. On the other hand, more power levels will lead to a higher computation complexity.

To study the impact of number of power levels, we run 1,000 experiments with both exponential power level sets and uniform power level sets, where the maximum number of power levels is 5. For each experiment, we run ARM1 with $\sigma = 0.05$ and 10^5 transitions.

Table 5 summarizes the algorithm performances with the exponential power level sets. We compare the ARM1 algorithm with the result obtained through exhaustive search (ES). The "ES Improvement" in the third row computes the ES performance difference between the current n and the previous $n-1$ power levels, where $n = 3, 4, 5$. The "ARM Improvement" in the fifth row is computed similarily. The last row records the absolute

TABLE 6
Performance Comparison for Uniform Power Level Sets

Number of Power Levels	2	3	4	5
ES (bit/s/Hz)	9.9337	10.3755	10.5683	10.6263
ES Improvement (bit/s/Hz)	–	0.4418	0.1928	0.0580
Performance Ratio	93.48%	97.64%	99.45%	100%
ARM (bit/s/Hz)	9.9241	10.3567	10.5418	10.5897
ARM Improvement (bit/s/Hz)	–	0.4326	0.1851	0.0479
Performance Ratio	93.71%	97.80%	99.54%	100%
Performance Gap	0.1%	0.18%	0.25%	0.34%

performance gap between ES and ARM under each choice of n. Table 6 summarizes the algorithm performances for the uniform power level sets. Note uniform and exponential power level sets are the same when $n = 2$ or $n = 3$.

Tables 5 and 6 illustrate the following common observations: (i) A large number of power levels leads to a better algorithm performance. (ii) The marginal performance improvement due to an additional power level quickly diminishes as n becomes large. (iii) The performance gap between ES and ARM slightly increases with n. We believe that this is due to the fact that we use the same stopping criterion (i.e., 10^5 transitions) for all experiments, but a larger n requires a longer convergence time to the stationary result of ARM. Intuitively, more power levels leads to a larger state space and a longer time to converge, and thus a higher complexity.

The above results imply that a relatively small number of fixed power levels can achieve a close-to-optimal performance with a low complexity. For example, four power levels should be good enough. Even having just two power levels can already achieve over 93 percent of the performance that can be achieved by using five power levels.

In addition, we also observe that for the same number of power levels, the uniform power level set has better performances than the exponential power level set.

4.4 Performance Comparison for 10-cell Network

In this subsection, we run 1,000 experiments for both ARM1 and ARM2 under the setting of $\sigma = 1$ and 0.2, 10^5 transitions per experiment and different uniform power level sets (power levels = 2, 3, 4, 5). Fig. 5 summarizes the average sum spectrum efficiencies and corresponding results (for the first 1,000 transitions). We can see ARM1 and ARM2 converges quickly and their performances are nearly the same (slightly differences at transient states).

4.5 Robustness of ARM

As we discussed in Section 3.1, ARM is robust to the inaccuracy of rating information. To validate this result, we consider a more complex cellular network (i.e., 61 cells in total) shown in Fig. 6. We run ARM algorithm with two options (ARM1 and ARM2) under the setting of $\sigma = 0.05$ and different uniform power level sets.

As shown in Fig. 6, we consider two scenarios. In one scenario, each cell only receives the rating information from its immediate neighboring cells, i.e., the first-hop cells. In the other scenario, each cell only receives the rating information

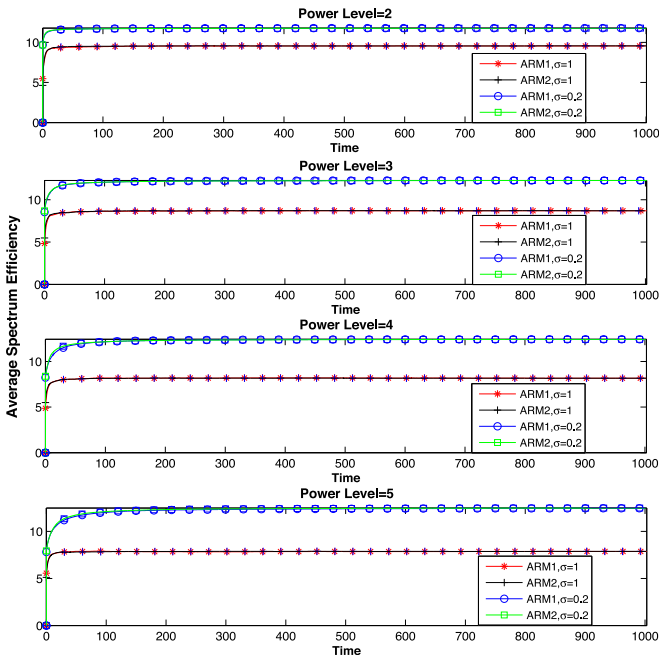

Fig. 5. Performance comparison for 10-cell network.

from both the first-hop and the second-hop cells. Any rating information from other cells will be ignored. The performances are shown in Tables 7 and 8 for ARM1 and ARM2 respectively.

We can see that in the worst-case scenario, ARM1 (ARM2) with only one-hop local rating information can still maintain more than 85 percent (81 percent) of the original performance without information loss. When two-hop local rating information is considered, the worse-case performance increases to over 93 percent (89 percent) of the original performance. The intuition is that the interference decreases with distance, hence the immediate neighboring cells' feedbacks are the most important ones, while the feedbacks from remote cells are less important. This property guarantees ARM's robustness, and will be useful for reducing communication

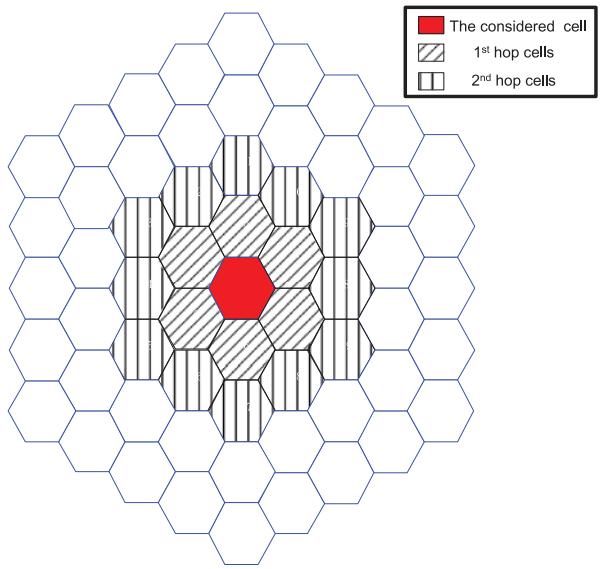

Fig. 6. 61-cell network.

TABLE 7
Impact of Information Loss: Average Performance of 2,000 Experiments for ARM1

	ARM1	ARM1 w./ 1-hop LR	ARM1 w./ 2-hop LR
2 power levels	66.2687	61.8718	65.0936
Performance Ratio	100%	93.37%	98.23%
3 power levels	68.6210	60.9217	66.2080
Performance Ratio	100%	88.78%	96.48%
4 power levels	69.6635	60.3204	65.8826
Performance Ratio	100%	86.59%	94.57%
5 power levels	70.1488	59.7764	65.3816
Performance Ratio	100%	85.21%	93.20%

TABLE 8
Impact of Information Loss: Average Performance of 2,000 Experiments for ARM2

	ARM2	ARM2 w./ 1-hop LR	ARM2 w./ 2-hop LR
2 power levels	66.3197	60.8498	64.7830
Performance Ratio	100%	91.75%	97.68%
3 power levels	68.7524	59.1214	64.9293
Performance Ratio	100%	85.99%	94.44%
4 power levels	69.8381	58.2431	63.8606
Performance Ratio	100%	83.40%	91.44%
5 power levels	70.3774	57.6095	63.0406
Performance Ratio	100%	81.86%	89.58%

complexity of ARM when implementing it in practical systems.

We also find that the less number of power levels, the better the performance of ARM with local rating. Intuitively, the larger number of power levels, the more sensitive the mapping from SINR to rate, and consequently the more perturbations due to the loss of the rating information. Comparatively, a smaller number of power levels is less insensitive to the information loss. For example, for two power levels, ARM1 (ARM2) with one-hop local rating already maintains more than 95 percent (91 percent) of the original performance.

By comparing the performances of ARM1 and ARM2, we find that on average, ARM2 performs slightly better than ARM1 for the case of non-local-rating. However, ARM1 performs better than ARM2 for the case of local-rating. Therefore, ARM1 is more robust than ARM2.

5 Proof for Theorem 2

Here we only show the case for ARM with option 1 (7). The proof of other case for ARM with option 2 (9) is similar and we omit the details.

(a) First, we present the mixing time bounds for the power-hopping Markov chain, which are obtained by the spectral analysis method [27]. Due to the space limit, we present the proof details in our technical report [21].

(b) Second, we present the mixing time bounds for the power-hopping Markov chain, which are obtained by the path coupling method [30].

We obtain a discrete-time Markov chain by uniformization of continuous-time power-hopping Markov chain. Denote this discrete-time Markov chain as $\mathcal{M}$. $\mathcal{M}$ is designed to sample from a given probability distribution π^* in (6) on a state space $\mathcal{P}$. At each step, it selects a link $v \in \mathcal{L}$ uniformly at random and adjusts its transmission power. More precisely, when Markov chain $\mathcal{M}$ resides in a feasible configuration $\boldsymbol{p} \in \mathcal{P}$, it does the following:

1) pick a link $w \in \mathcal{L}$ uniformly at random (with probability $\frac{1}{L}$), and denote its assigned power level as $p_w(\boldsymbol{p})$;
2) pick a new power level $p_w(\boldsymbol{p}')$ uniformly at random (with probability $\frac{1}{n}$);
3) with probability $\frac{\exp\left(\frac{1}{\sigma}\left(\sum_{l\in\mathcal{L}} R_{l|\boldsymbol{p}'}\right)\right)}{\exp\left(\frac{1}{\sigma}\left(\sum_{l\in\mathcal{L}} R_{l|\boldsymbol{p}}\right)\right)+\exp\left(\frac{1}{\sigma}\left(\sum_{l\in\mathcal{L}} R_{l|\boldsymbol{p}'}\right)\right)}$, link w sets its transmission power level to be $p_w(\boldsymbol{p}')$, otherwise it switches back to the previous power level $p_w(\boldsymbol{p})$.

Thus $\mathcal{M}$ has a transition matrix $M = I + Q/\theta'$, where I is the identity matrix and

$$\theta' = L \cdot n \cdot C. \tag{47}$$

We can see that $\mathcal{M}$ is indeed a uniformized version of power-hopping Markov chain.

Now we apply the coupling method to bound the mixing time of $\mathcal{M}$. By a "coupling" for this chain, we mean considering a joint stochastic process (X_t, Y_t) on $\mathcal{P} \times \mathcal{P}$, such that each of the processes (X_t) and (Y_t) is a Markov chain on $\mathcal{P}$ with the transition matrix M. Typically, after defining the distance metric $d : \mathcal{P} \times \mathcal{P} \to \{0, 1, \ldots, d_{\max}\}$, we try to construct a one-step distance-decreasing coupling $(X_0, Y_0) \to (X_1, Y_1)$ such that

$$E(d(X_1, Y_1)|X_0, Y_0) \leq \lambda \cdot d(X_0, Y_0), \tag{48}$$

for all $(X_0, Y_0) \in \mathcal{P} \times \mathcal{P}$, where $0 \leq \lambda < 1$. Applying this coupling iteratively results in a t-step coupling and a mixing time analysis.

In general, defining and analyzing a coupling for all pairs $X_t, Y_t \in \mathcal{P}$ is difficult. The path coupling technique [30] simplifies the approach by restricting attention to pairs in a connected subset $S \subseteq \mathcal{P} \times \mathcal{P}$. It then suffices to define a one-step coupling, such that (48) holds for all $(X_0, Y_0) \in S$. Then the path coupling theorem [30] constructs, via simple compositions, a one-step coupling satisfying (48) for all $X_0, Y_0 \in \mathcal{P}$.

Given any two configurations $X, Y \in \mathcal{P}$, let $d(X, Y)$ denote the Hamming distance between X and Y, which equals to the number of links at which the chosen power levels are different. Now we denote S as configuration pairs $X, Y \in \mathcal{P}$, such that the power configurations differ at exactly one link. Then we have

$$S = \{(X, Y) \in \mathcal{P} \times \mathcal{P} : d(X, Y) = 1\}. \tag{49}$$

For any link $v \in \mathcal{L}$, we denote v^X as the chosen power level under configuration X. For example, if link v chooses power level c under X, then $v^X = c$. Now we design a one-step coupling.

More precisely, consider a configuration pair $(X_0, Y_0) \in S$. Without loss of generality, we have

$$X_0 = (v_1^{X_0}, \ldots, v_L^{X_0}), \tag{50}$$

$$Y_0 = (v_1^{Y_0}, \ldots, v_L^{Y_0}), \tag{51}$$

where $v_j^{X_0} = v_j^{Y_0}, \forall j = 2, \ldots, L$, and

$$v_1^{X_0} = a \in \mathcal{P}, \tag{52}$$

$$v_1^{Y_0} = b \in \mathcal{P} - \{a\}. \tag{53}$$

A link $w \in \mathcal{L}$ is chosen uniformly at random. At every step, both chains update the same link w. Note there are $n+1$ power levels denoted by $\mathcal{P} = \{P_0, P_1, \ldots, P_n\}$. Without loss of generality, we assume $a = P_1$ and $b = P_2$. Let $w^{X_0}(+)$ $\left(w^{Y_0}(+), respectively\right)$ denote the power level that link w selects and switches to under X_0 (Y_0, respectively). Here $w^{X_0}(+) = w^{X_0}$ ($w^{Y_0}(+) = w^{Y_0}$, respectively) means link w does not switch the power level under X_0 (Y_0, respectively).

The coupling for the update at time 1 is $(X_0, Y_0) \to (X_1, Y_1)$, where $(X_0, Y_0) \to (X_1, Y_1)$ denotes the power level switching operation. Then the coupling is shown as follows:

(1). if $w \neq v_1$, without loss of generality, we assume $w = v_j, 2 \leq j \leq L$ and we have $w^{X_0} = w^{Y_0} = P_m, 0 \leq m \leq n$. We denote $p_{k,j} = Pr(w^{X_0}(+) = P_k)$ and $q_{k,j} = Pr(w^{Y_0}(+) = P_k), 0 \leq k \leq n$. Then we have

$$\begin{aligned} p_{m,j} &= Pr(w^{X_0}(+) = P_m), \\ &= \frac{\exp\left(\frac{1}{\sigma}\left(\sum_{l\in\mathcal{L}} R_{lX_0}\right)\right)}{\exp\left(\frac{1}{\sigma}\left(\sum_{l\in\mathcal{L}} R_{lX_0}\right)\right) + \exp\left(\frac{1}{\sigma}\left(\sum_{l\in\mathcal{L}} R_{lX_1}\right)\right)}; \end{aligned} \tag{54}$$

$$\begin{aligned} &\text{for all} \quad 0 \leq k \leq n, k \neq m, \\ &p_{k,j} = Pr(w^{X_0}(+) = P_k), \\ &\quad = \frac{1}{n} \cdot \frac{\exp\left(\frac{1}{\sigma}\left(\sum_{l\in\mathcal{L}} R_{lX_1}\right)\right)}{\exp\left(\frac{1}{\sigma}\left(\sum_{l\in\mathcal{L}} R_{lX_0}\right)\right) + \exp\left(\frac{1}{\sigma}\left(\sum_{l\in\mathcal{L}} R_{lX_1}\right)\right)}; \end{aligned} \tag{55}$$

$$\begin{aligned} q_{m,j} &= Pr(w^{Y_0}(+) = P_m), \\ &= \frac{\exp\left(\frac{1}{\sigma}\left(\sum_{l\in\mathcal{L}} R_{lY_0}\right)\right)}{\exp\left(\frac{1}{\sigma}\left(\sum_{l\in\mathcal{L}} R_{lY_0}\right)\right) + \exp\left(\frac{1}{\sigma}\left(\sum_{l\in\mathcal{L}} R_{lY_1}\right)\right)}; \end{aligned} \tag{56}$$

$$\begin{aligned} &\text{and for all} \quad 0 \leq k \leq n, k \neq m, \\ &q_{k,j} = Pr(w^{Y_0}(+) = P_k), \\ &\quad = \frac{1}{n} \cdot \frac{\exp\left(\frac{1}{\sigma}\left(\sum_{l\in\mathcal{L}} R_{lY_1}\right)\right)}{\exp\left(\frac{1}{\sigma}\left(\sum_{l\in\mathcal{L}} R_{lY_0}\right)\right) + \exp\left(\frac{1}{\sigma}\left(\sum_{l\in\mathcal{L}} R_{lY_1}\right)\right)}. \end{aligned} \tag{57}$$

We then take $r_{k,j} = \min\{p_{k,j}, q_{k,j}\}$ for any $k \in \{0, \ldots, n\}$. Now we define a random variable H_j satisfying

$$Pr(H_j = k) = \begin{cases} r_{k,j} & \text{if } 0 \leq k \leq n \\ 1 - \sum_{i=0}^{n} r_{i,j} & \text{if } k = n+1 \\ 0 & \text{otherwise.} \end{cases}$$

We update X_0, Y_0 according to the following rules.

1) If $H_j = k$ where $0 \leq k \leq n$, then $w^{X_0}(+) = w^{Y_0}(+) = P_k$.
2) If $H_j = n+1$, then update X_0, Y_0 independently.
   a) $Pr(w^{X_0}(+) = P_k | H_j = n+1) = \frac{p_{k,j} - r_{k,j}}{1 - \sum_{i=0}^{n} r_{i,j}}$, $\forall k \in \{0, \ldots, n\}$.
   b) $Pr(w^{Y_0}(+) = P_k | H_j = n+1) = \frac{q_{k,j} - r_{k,j}}{1 - \sum_{i=0}^{n} r_{i,j}}$, $\forall k \in \{0, \ldots, n\}$.

(2) Otherwise, $w = v_1$. We have

$$w^{X_0} = a \in \mathcal{P}, \tag{58}$$

$$w^{Y_0} = b \in \mathcal{P} - \{a\}. \tag{59}$$

Here $w^{X_0}(+) = a$ ($w^{Y_0}(+) = b$, respectively) means link w does not adjust the transmission power under X_0 (Y_0, respectively). We denote $p_{k,1} = Pr(w^{X_0}(+) = P_k)$ and $q_{k,1} = Pr(w^{Y_0}(+) = P_k), 0 \leq k \leq n$. We have

$$\begin{aligned} p_{1,1} &= Pr(w^{X_0}(+) = P_1 = a), \\ &= \frac{\exp\left(\frac{1}{\sigma}\left(\sum_{l\in\mathcal{L}} R_{lX_0}\right)\right)}{\exp\left(\frac{1}{\sigma}\left(\sum_{l\in\mathcal{L}} R_{lX_0}\right)\right) + \exp\left(\frac{1}{\sigma}\left(\sum_{l\in\mathcal{L}} R_{lX_1}\right)\right)}; \end{aligned} \tag{60}$$

$$\begin{aligned} &\text{for all} \quad k \in \{0, 2, \ldots, n\}, \\ &p_{k,1} = Pr(w^{X_0}(+) = P_k), \\ &\quad = \frac{1}{n} \cdot \frac{\exp\left(\frac{1}{\sigma}\left(\sum_{l\in\mathcal{L}} R_{lX_1}\right)\right)}{\exp\left(\frac{1}{\sigma}\left(\sum_{l\in\mathcal{L}} R_{lX_0}\right)\right) + \exp\left(\frac{1}{\sigma}\left(\sum_{l\in\mathcal{L}} R_{lX_1}\right)\right)}; \end{aligned} \tag{61}$$

$$\begin{aligned} q_{2,1} &= Pr(w^{Y_0}(+) = P_2 = b), \\ &= \frac{\exp\left(\frac{1}{\sigma}\left(\sum_{l\in\mathcal{L}} R_{lY_0}\right)\right)}{\exp\left(\frac{1}{\sigma}\left(\sum_{l\in\mathcal{L}} R_{lY_0}\right)\right) + \exp\left(\frac{1}{\sigma}\left(\sum_{l\in\mathcal{L}} R_{lY_1}\right)\right)}; \end{aligned} \tag{62}$$

$$\begin{aligned} &\text{and for all} \quad k \in \{0, 1, 3, \ldots, n\}, \\ &q_{k,1} = Pr(w^{Y_0}(+) = P_k), \\ &\quad = \frac{1}{n} \cdot \frac{\exp\left(\frac{1}{\sigma}\left(\sum_{l\in\mathcal{L}} R_{lY_1}\right)\right)}{\exp\left(\frac{1}{\sigma}\left(\sum_{l\in\mathcal{L}} R_{lY_0}\right)\right) + \exp\left(\frac{1}{\sigma}\left(\sum_{l\in\mathcal{L}} R_{lY_1}\right)\right)}. \end{aligned} \tag{63}$$

We then take $r_{k,1} = \min\{p_{k,1}, q_{k,1}\}$ for any $k \in \{0, \ldots, n\}$. Now we define a random variable H_1 satisfying

$$Pr(H_1 = k) = \begin{cases} r_{k,1} & \text{if } 0 \leq k \leq n \\ 1 - \sum_{i=0}^{n} r_{i,1} & \text{if } k = n+1 \\ 0 & \text{otherwise.} \end{cases}$$

We update X_0, Y_0 according to the following rules.

1) If $H_1 = k$ where $0 \leq k \leq n$, then $w^{X_0}(+) = w^{Y_0}(+) = P_k$.
2) If $H_1 = n+1$, then update X_0, Y_0 independently.
   a) $Pr(w^{X_0}(+) = P_k | H_1 = n+1) = \frac{p_{k,1} - r_{k,1}}{1 - \sum_{i=0}^{n} r_{i,1}}$, $\forall k \in \{0, \ldots, n\}$.
   b) $Pr(w^{Y_0}(+) = P_k | H_1 = n+1) = \frac{q_{k,1} - r_{k,1}}{1 - \sum_{i=0}^{n} r_{i,1}}$, $\forall k \in \{0, \ldots, n\}$.

We can see that the one-step coupling designed above is a valid coupling. Now we analyze the distance metric $E(d(X_1, Y_1) - 1 | X_0, Y_0)$.

By the above coupling we know that when $w = v_j, 1 \leq j \leq L$, $Pr(w^{X_0}(+) = w^{Y_0}(+)) = \sum_{i=0}^{n} r_{i,j}$. Then we have

$$E[d(X_1,Y_1)-1|X_0,Y_0,w=v_1]=-\sum_{i=0}^{n} r_{i,1}, \tag{64}$$

$$E[d(X_1,Y_1)-1|X_0,Y_0,w=v_j]=1-\sum_{i=0}^{n} r_{i,j}, \forall 2\le j\le L. \tag{65}$$

It follows that

$$E[d(X_1,Y_1)-1|X_0,Y_0], \tag{66}$$

$$=\sum_{j=1}^{L} P(w=v_j)\cdot E[d(X_1,Y_1)-1|X_0,Y_0,w=v_j], \tag{67}$$

$$=\frac{1}{L}\cdot\left[L-1-\sum_{j=1}^{L}\sum_{i=0}^{n} r_{i,j}\right]. \tag{68}$$

On the other hand we can see that

$$\sum_{i=0}^{n} r_{i,1}\ge\frac{n+1}{n}\cdot\frac{1}{1+\exp\left(\frac{\bar{L}\cdot r_m}{\sigma}\right)}, \tag{69}$$

$$\sum_{i=0}^{n} r_{i,j}\ge\frac{2}{1+\exp\left(\frac{\bar{L}\cdot r_m}{\sigma}\right)}, \forall 2\le j\le L, \tag{70}$$

where $\bar{L}\le L$ denotes the maximal number of links whose rates are changed due to one link's adjustment of power levels.

Therefore,

$$E[d(X_1,Y_1)-1|X_0,Y_0], \tag{71}$$

$$=\frac{1}{L}\cdot\left[L-1-\sum_{n=1}^{L}\sum_{j=1}^{M} r_{j,n}\right], \tag{72}$$

$$\le\frac{-K}{L}, \tag{73}$$

where

$$K=\frac{L+\frac{1}{n}+(1-L)\cdot\exp\left(\frac{\bar{L}\cdot r_m}{\sigma}\right)}{1+\exp\left(\frac{\bar{L}\cdot r_m}{\sigma}\right)}. \tag{74}$$

We can see $K>0$ for any

$$\sigma>\frac{L\cdot r_m}{\ln(1+\frac{1+1/n}{L-1})}\ge\frac{\bar{L}\cdot r_m}{\ln(1+\frac{1+1/n}{L-1})}. \tag{75}$$

Then it follows that for any $(X_0,Y_0)\in S$

$$E[d(X_1,Y_1)|X_0,Y_0]<1-\frac{K}{L}, \tag{76}$$

$$=(1-\frac{K}{L})\cdot d(X_0,Y_0). \tag{77}$$

By the path coupling theorem [30], we know that for any $(X_0,Y_0)\in\mathcal{P}\times\mathcal{P}$,

$$E[d(X_1,Y_1)|X_0,Y_0]<(1-\frac{K}{L})\cdot d(X_0,Y_0), \tag{78}$$

$$=\lambda\cdot d(X_0,Y_0). \tag{79}$$

where $\lambda=1-\frac{K}{L}$.

Applying this one-step coupling iteratively results in a t-step coupling, and we have for any t, $(X_t,Y_t)\in\mathcal{P}\times\mathcal{P}$,

$$P[X_t\ne Y_t]=P[d(X_t,Y_t)\ge 1], \tag{80}$$

$$\le E[d(X_t,Y_t)], \tag{81}$$

$$\le\lambda^t\cdot\text{diam}\,(\mathcal{P}), \tag{82}$$

$$\le L\cdot\lambda^t. \tag{83}$$

Thus for discrete-time Markov chain $\mathcal{M}$,

$$||M^t(X_0,\cdot)-M^t(Y_0,\cdot)||_{TV}\le L\cdot\lambda^t. \tag{84}$$

Then by (47), (74) and uniformization theorem [29], we know that for any $\boldsymbol{p}\in\mathcal{P}$,

$$||\pi_t(\boldsymbol{p})-\pi^*||_{TV}, \tag{85}$$

$$=||\sum_{j=0}^{\infty}\frac{(\theta' t)^j}{j!}\exp(-\theta' t)M^j(\boldsymbol{p},\cdot)-\pi^*||_{TV}, \tag{86}$$

$$\le\sum_{j=0}^{\infty}\frac{(\theta' t)^j}{j!}\exp(-\theta' t)||M^j(\boldsymbol{p},\cdot)-\pi^*||_{TV}, \tag{87}$$

$$\le L\cdot\sum_{j=0}^{\infty}\frac{(\theta' t\lambda)^j}{j!}\exp(-\theta' t), \tag{88}$$

$$=L\cdot\exp(-\theta'(1-\lambda)t), \tag{89}$$

$$=L\cdot\exp\left(-\theta'\cdot\frac{Kt}{L}\right), \tag{90}$$

$$=L\cdot\exp(-n\cdot C\cdot K\cdot t). \tag{91}$$

Thus we have

$$t_{mix}(\epsilon)\le\frac{\ln\frac{L}{\epsilon}}{n\cdot C}\cdot\frac{1+\exp\left(\frac{\bar{L}\cdot r_m}{\sigma}\right)}{L+\frac{1}{n}-(L-1)\exp\left(\frac{\bar{L}\cdot r_m}{\sigma}\right)}. \tag{92}$$

(c) By (92) and (75) we can see that given $\sigma_{th}^1=\frac{L\cdot r_m}{\ln(1+\frac{1+1/n}{L-1})}$, if $\sigma>\sigma_{th}^1$, the upper bound of mixing time is $t_{\text{mix}}(\epsilon)\sim O\big(\exp(\frac{1}{\sigma})\cdot\ln\frac{L}{\epsilon}\big)$. Otherwise when $0<\sigma\le\sigma_{th}^1$, the upper bound of mixing time is $t_{\text{mix}}(\epsilon)\sim\Omega(\exp\left(\frac{L}{\sigma}+\ln\ln\frac{1}{\epsilon}\right))$, which completes the proof.

6 Conclusions

In this paper we propose ARM, a novel distributed algorithm framework to solve the discrete power control problem, under the physical interference model and the practical setting of limited numbers of power levels and modulation-coding schemes. By both mathematical analysis and extensive simulations, we show that ARM can achieve

close-to-optimal performances. Moreover, this algorithm is simple and robust, and thus shows great potentials for interference management in practical wireless systems. We provide two options of ARM, which achieve similar performance in most simulation settings. When facing the possibility of rating information loss due to locality, ARM1 is more robust and ARM2 has a slightly better performance.

There are several interesting directions for future research, including the extension to multi-channel-per-link scenario, new error model for the study of robustness, the design of optimal power level set, the characterization of the impact of information loss for general network topology, and the extension of ARM for time-variant networking environments.

Acknowledgments

This work was partially supported by a NSFC grant (No. 61302114), and the General Research Funds (Project Number CUHK 412713 and 14202814) established under the University Grant Committee of the Hong Kong Special Administrative Region, China. Part of the results have appeared in the *Proceeding of the WiOpt Conf.* [1].

References

[1] S. Li, Z. Shao, and J. Huang, "ARM: Anonymous rating mechanism for discrete power control," in *Proc. 13th Int. Symp. Modeling Optim. Mobile, Ad Hoc Wireless Netw. (WiOpt)*, May 2015, pp. 199–206.

[2] M. Chiang, P. Hande, T. Lan, and C. W. Tan, "Power control in wireless cellular networks," *Foundations Trends Netw.*, vol. 2, no. 4, pp. 381–533, 2008.

[3] G. J. Foschini and Z. Miljanic, "A simple distributed autonomous power control algorithm and its convergence," *IEEE Trans. Veh. Technol.*, vol. 42, no. 4, pp. 641–646, Nov. 1993.

[4] R. D. Yates, "A framework for uplink power control in cellular radio systems," *IEEE J. Selected Areas Commun.*, vol. 13, no. 7, pp. 1341–1347, Sep. 1995.

[5] L. Qian, Y. J. Zhang, and J. Huang, "Mapel: Achieving global optimality for a non-convex wireless power control problem," *IEEE Trans. Wireless Commun.*, vol. 8, no. 3, pp. 1553–1563, Mar. 2009.

[6] J. Huang, R. A. Berry, and M. L. Honig, "Distributed interference compensation for wireless networks," *IEEE J. Selected Areas Commun.*, vol. 24, no. 5, pp. 1074–1084, Sep. 2006.

[7] P. Hande, S. Rangan, M. Chiang, and X. Wu, "Distributed uplink power control for optimal sir assignment in cellular data networks," *IEEE/ACM Trans. Netw.*, vol. 16, no. 6, pp. 1420–1433, Dec. 2008.

[8] L. P. Qian, Y. J. Zhang, and M. Chiang, "Globally optimal distributed power control for nonconcave utility maximization," in *Proc. IEEE Global Telecommun. Conf.*, Dec., 2010, pp. 1–6.

[9] S. Sesia, I. Toufik, and M. Baker, *LTE: The UMTS Long Term Evolution*. Hoboken, NJ, USA: Wiley, 2009.

[10] S. Zhou, X. Wu, and L. Ying, "Distributed power control and coding-modulation adaptation in wireless networks using annealed Gibbs sampling," in *Proc. IEEE 31st Annu. Int. Conf. Comput. Commun. Mini-Conf.*, Mar. 2012, pp. 3016–3020.

[11] C. Wu and D. P. Bertsekas, "Distributed power control algorithms for wireless networks," *IEEE Trans. Veh. Technol.*, vol. 50, no. 2, pp. 504–514, Mar. 2001.

[12] C. W. Sung and W. S. Wong, "A distributed fixed-step power control algorithm with quantization and active link quality protection," *IEEE Trans. Veh. Technol.*, vol. 48, no. 2, pp. 553–562, Mar. 1999.

[13] A. Gjendemsjø, D. Gesbert, G. E. Oien, and S. G. Kiani, "Binary power control for sum rate maximization over multiple interfering links," *IEEE Trans. Wireless Commun.*, vol. 7, no. 8, pp. 3164–3173, Aug. 2008.

[14] H. Zhang, L. Venturino, N. Prasad, P. Li, S. Rangarajan, and X. Wang, "Weighted sum-rate maximization in multi-cell networks via coordinated scheduling and discrete power control," *IEEE J. Selected Areas Commun.*, vol. 29, no. 6, pp. 1214–1224, Jun. 2011.

[15] D. Wang, X. Xu, X. Chen, X. Tao, Y. Yin, and H. Haas, "Discrete power allocation via ant colony optimization for multi-cell OFDM systems," in *Proc. IEEE Veh. Technol. Conf. Fall*, Sep. 2012, pp. 1–5.

[16] R. Combes, A. Proutiere, D. Yun, J. Ok, and Y. Yi, "Optimal rate sampling in 802.11 systems," in *Proc. IEEE INFOCOM*, 2014, pp. 2760–2767.

[17] Y. Xing and R. Chandramouli, "Stochastic learning solution for distributed discrete power control game in wireless data networks," *IEEE/ACM Trans. Netw.*, vol. 16, no. 4, pp. 932–944, Aug. 2008.

[18] S. M. Perlaza, H. Tembine, and S. Lasaulce, "How can ignorant but patient cognitive terminals learn their strategy and utility?" in *Proc. IEEE 11th Int. Workshop Signal Process. Adv. Wireless Commun.*, 2010, pp. 1–5.

[19] S. M. Perlaza, H. Tembine, S. Lasaulce, and M. Debbah, "Quality-of-service provisioning in decentralized networks: A satisfaction equilibrium approach," *IEEE J. Selected Topics Signal Process.*, vol. 6, no. 2, pp. 104–116, Apr. 2012.

[20] W. Zhong, G. Chen, S. Jin, and K.-K. Wong, "Relay selection and discrete power control for cognitive relay networks via potential game," *IEEE Trans. Signal Process.*, vol. 62, no. 20, pp. 5411–5424, Oct. 2014.

[21] S. Li, Z. Shao, and J. Huang. (2016). Arm: Anonymous rating mechanism for discrete power control [Online]. Available: https://www.dropbox.com/s/iomgfjdgshovp9h/ARM-report.pdf

[22] 3gpp tr 36.814. (2010). *The Mobile Broadband Standard* [Online]. Available: http://www.3gpp.org/DynaReport/36814.htm

[23] Z.-Q. Luo and S. Zhang, "Dynamic spectrum management: Complexity and duality," *IEEE J. Selected Topics Signal Process.*, vol. 2, no. 1, pp. 57–73, Feb. 2008.

[24] M. Chen, S. Liew, Z. Shao, and C. Kai, "Markov approximation for combinatorial network optimization," *IEEE Trans. Inform. Theory*, vol. 59, no. 10, pp. 6301–6327, Oct. 2013.

[25] L. Jiang and J. Walrand, "A distributed CSMA algorithm for throughput and utility maximization in wireless networks," *IEEE/ACM Trans. Netw.*, vol. 18, no. 3, pp. 960–972, Jun. 2010.

[26] M. Andrews and L. Zhang, "Utility optimization in heterogeneous networks via CSMA-based algorithms," in *Proc. 11th Int. Symp. Model. Optim. Mobile, Ad Hoc Wireless Netw.*, May 2013, pp. 372–379.

[27] P. Diaconis and D. Stroock, "Geometric bounds for eigenvalues of Markov chains," *Annal. Appl. Probability*, vol. 1, no. 1, pp. 36–61, 1991.

[28] S. Zhang, Z. Shao, and M. Chen, "Optimal distributed P2P streaming under node degree bounds," in *Proc. IEEE 18th Int. Conf., Netw. Protocols*, Oct. 2010, pp. 253–262.

[29] D. A. Levin, Y. Peres, and E. L. Wilmer, *Markov Chains and Mixing Times*. Providence, RI, USA: American Mathematical Soc., 2009.

[30] R. Bubley and M. Dyer, "Path coupling: A technique for proving rapid mixing in markov chains," in *Proc. IEEE 54th Annu. Symp. Foundations Comput. Sci.*, Oct. 1997, pp. 223–231.

Shuqin Li received the PhD degree in information engineering from the Chinese University of Hong Kong, Hong Kong, in 2012. Currently, she is working as a research scientist with Bell Labs Shanghai, Alcatel-Lucent Shanghai Bell Co., Ltd., Shanghai, China. Her research interests include resource allocation, pricing and revenue management in communication networks, applied game theory, contract theory and incentive mechanism design in network economics, network coding, and stochastic network optimization. She is a member of the IEEE.

Ziyu Shao the BS and ME degrees in electrical engineering from the Peking University, Beijing, China, and the PhD degree in information engineering from the Chinese University of Hong Kong, Shatin, N.T., Hong Kong. He is an assistant professor in the School of Information Science and Technology, ShanghaiTech University, Shanghai, China. He worked as a postdoctoral fellow at the Institute of Network Coding, The Chinese University of Hong Kong, Shatin, N.T., Hong Kong, during 2011-2013. His research interests include distributed algorithm and system design, network optimization, mobile computing, and cloud computing. He is a member of the IEEE.

Jianwei Huang received the PhD degree from Northwestern University in 2005, and worked as a postdoctoral research associate at Princeton University during 2005-2007. He is an associate professor and the director of the Network Communications and Economics Lab (ncel.ie.cuhk.edu.hk), Department of Information Engineering, Chinese University of Hong Kong. He received eight international Best Paper Awards, including the IEEE Marconi Prize Paper Award in Wireless Communications in 2011. He has co-authored four books: *Wireless Network Pricing*, *Monotonic Optimization in Communication and Networking Systems*, *Cognitive Mobile Virtual Network Operator Games*, and *Social Cognitive Radio Networks*. He has served as an associate editor of the *IEEE Transactions on Cognitive Communications and Networking, IEEE Transactions on Wireless Communications, and IEEE Journal on Selected Areas in Communications - Cognitive Radio Series*. He is the vice chair of the IEEE ComSoc Cognitive Network Technical Committee and the past chair of the IEEE ComSoc Multimedia Communications Technical Committee. He is a distinguished lecturer of the IEEE Communications Society. He is a fellow of the IEEE.

▷ **For more information on this or any other computing topic, please visit our Digital Library at** www.computer.org/publications/dlib.